

**Advanced Materials  
and Application**

International Symposium on Advanced  
Materials and Application (ISAMA 2018)

Edited by  
Prof. Mitesh Katarop

## Mechanical and Electrical Technology VII

<b>Papers</b>		<b>Book</b>	Volumes 799-800
<input type="text" value="Search"/>		doi: <a href="https://doi.org/10.4028/www.scientific.net/AMM.799-800">https://doi.org/10.4028/www.scientific.net/AMM.799-800</a>	
		<a href="#">&lt;</a> <a href="#">1</a> <a href="#">2</a> <a href="#">3</a> <a href="#">4</a> <a href="#">5</a> <a href="#">...</a> <a href="#">&gt;</a> <a href="#">&gt;&gt;</a>	
Paper Title			Page
<b><u>Synthesis of ZrO<sub>2</sub> Nanotubes by Anodization of Zr Foil</u></b>			125
Authors: Mary Donnabelle L. Balela, April Alexa S. Lagarde, Stephen Jann A. Tamayo, Nikko S. Villareal, Ann Marielle Parreno			
Abstract: Zirconia (ZrO <sub>2</sub> ) nanotubes were synthesized by anodization of zirconium (Zr) foil in NH <sub>4</sub> F and (NH <sub>4</sub> ) <sub>2</sub> SO <sub>4</sub> aqueous solution. Different surface preparation methods			
<a href="#">...more</a>			
-----			
<b><u>Use of Classification Trees and Rule-Based Methods to Predict Shapes of Nano-Aggregates of Reinforcement Fillers</u></b>			130
Authors: R. Fernandez-Martinez, Pello Jimbert, M. Iturrondobeitia, J. Ibarretxe, T. Guraya-Díez			
Abstract: While manufacturing composite materials, reinforcement fillers inevitable collide with each other and subsequently they congregate to aggregates with different			
<a href="#">...more</a>			
-----			
<b><u>Compressive Behaviour of Low Density Polymeric Syntactic Foams</u></b>			135
Authors: Zulzamri Salleh, Md Mainul Islam, Jayantha Ananda Epaarachchi			
Abstract: The combinations of polymer resin and glass microballoon are the main materials used to produce syntactic foams. Syntactic foam is a lightweight material that			
<a href="#">...more</a>			
-----			
<b><u>Adhesion Phenomenon of Titanium as Cathode in Aluminum Anodizing</u></b>			140
Authors: Putu Hadi Setyarini, Rudy Soenoko, Agus Suprpto, Yudy Surya Irawan			
Abstract: This paper discusses the film coating formation mechanism after an anodizing process carried out in AA6061 with a varying potential between 15-30V. The			
<a href="#">...more</a>			

## Adhesion Phenomenon of Titanium as Cathode in Aluminum Anodizing

PutuHadi Setyarini<sup>1,2,a</sup>, Rudy Soenoko<sup>2,b</sup>, Agus Suprpto<sup>3,c</sup>  
and Yudy Surya Irawan<sup>2,d</sup>

<sup>1</sup>Doctoral Student of Department of Mechanical Engineering, Faculty of Engineering, Brawijaya University, Malang, Indonesia 65145

<sup>2</sup>Department of Mechanical Engineering, Faculty of Engineering, Brawijaya University, Malang, Indonesia 65145

<sup>3</sup>Department of Mechanical Engineering, Faculty of Engineering, Merdeka University, Malang, Indonesia 65115

<sup>a</sup>putu\_hadi@ub.ac.id, <sup>b</sup>rudysoen@ub.ac.id, <sup>c</sup>agus.suprpto@unmer.ac.id, <sup>d</sup>yudysir@ub.ac.id

**Keywords:** Titanium Adhesion; Anodizing of AA6061; Potential.

**Abstract.** This paper discusses the film coating formation mechanism after an anodizing process carried out in AA6061 with a varying potential between 15-30V. The electrolyte used to be 1M H<sub>3</sub>PO<sub>4</sub> with titanium as the cathode. From this study, it was found that after the anodizing process the pore uniformity occurs with a size varied from 1.09-5.74 μm become 2.78-4.56 μm. There was also an increase in the titanium content on the deposition surface about 21% and was achieved at an electric potential of 25V where titanium in the pore penetration occurs up to the depth of 5 μm.

### Introduction

Anodizing is the most widely used for surface treatment process in aluminum because it can improve material wear and corrosion resistance and it can be applied to many fields [1-4]. In this process, the oxide layer is formed as a barrier layer on the inside layer of thin layers, while on a thicker layer there will be much porous [5-6]. Pores form in the oxide layer is affected by the coating quality and it is also influenced by the electric potential applied during the process [7].

The use of different materials as the cathode in order to strengthen the oxide layer on the anodizing process has pretty much done. Allam and Grimes examined the effectiveness of the use of titanium as the anode for some cathode materials to find out how it can affect the architectural form of the nanotube cathode besides looking for a cheaper alternative of cathode [8]. Meanwhile, several different metals that have been used as cathodes in aluminum anodizing process are stainless steel [9], titanium [10] and lead [11]. Another research was also used magnesium as the anode and combined with stainless steel as the cathode [12]. It is used because we know that metal electrode would affect the reaction step rate and surely would influence the overall anodizing performance results [8]. Zhang *et. al.* also stated that the film layer with two types of particles would increase the mechanical properties and also the wear and corrosion resistance [9].

In this study, the process of titanium adhesion was investigated, therefore titanium is positioned as a cathode material in AA6061. The electrical potential used was in the range between 15-30V with 1M H<sub>3</sub>PO<sub>4</sub> as the electrolyte solution. Anodizing parameters would influence the potency of forming the pore pattern, pore size and titanium penetration depth will be discussed further. This study offers a fundamental understanding of the anodizing process that may be applied to nanotechnology, especially in the field of medical technology.

### Experimental Method

The material used in this experiment was AA6061 with a size of 50 mm x 6 mm x 6 mm. The alloy composition included 0.4% Si, 0.8% Mg, 0.7% Fe, 0.15% Cu, 0.25% Zn, 0.15% Ti, 0.15% Mn, 0.04 % Cr, Al was balanced. Titanium was used as the cathode with a composition included 2.6% P,

2.43% Ca, 0.54% Fe, 92.2% Ti, 0.29% Ni, 0.14% Zn, 0.90% Tm, with a size of 90 mm × 90 mm × 0.5 mm.

The initial treatment given to the material before anodized by polishing the specimen surface using a sand paper to get a mirror like surface. The next step was degreasing the material surface using a solution of 15% H<sub>2</sub>SO<sub>4</sub> at 60 ± 10<sup>0</sup>C for 10 minutes, cleaning using NaOH at 50 ± 10<sup>0</sup>C for 10 minutes and finally followed by desmutting in a 10% HNO<sub>3</sub> at 30 ± 10<sup>0</sup>C for 5 minutes. Anodizing process was performed using an electrolyte solution of 1M H<sub>3</sub>PO<sub>4</sub>. Electrolyte temperature was kept constant at 0 ± 5<sup>0</sup>C with a distance of 5 cm between the anode and the cathode and 60 minutes of processing time under an electrical potential of 15-30V.

The characterization after the process was done by using the Scanning Electron Microscope (SEM). The elemental analysis was performed using an Energy Dispersive X-ray (EDX).

## Result and Discussion

Layers formed on the specimen surface were characterized using SEM, with emphasizing on material surface morphology and cross-sectional side. Figure 1 (a) shows the results of the anodizing at an electric potential of 15 V, where the pores are formed not uniformly and the pore size were varies between 1.09 - 5.74 μm. The pores formed also seem not evenly spread over the whole specimen. Meanwhile Figure 1 (b) shows that the specimen after anodized at an electrical potential of 20 V shows that the pore distribution began more uniform on the specimen surface with a size range between 1.20 - 5.03 μm.

The pore size is between 1.57 - 3.88 μm which is shown in Figure 1 (c), this was the result of anodizing with an electric potential of 25V. Pits began to appear in some parts of the specimen surface. However anodizing potential showed the resulting pore size began to have a uniform size. Whereas Figure 1 (d) showed the pore formed in the anodizing results in an electrical potential of 30 V had the same relative size to those produced by the electrical potential of 25V which is 2.78 - 4.56 μm. It seems that many big pits appear on the specimen surface. The pit may appear because of the loss of particles and attacks the pore lining [12].

It can be seen that the overall morphology of the specimen surface showed the same characteristic. Like the pores on the anodizing coating surface which has a different size and distributed unevenly on AA 6061 surface layer which has been anodized. it can be concluded that the electrical potential and the cathode material play an important role in the appearance of surface precipitates. An increase in the electrical potential would increase the current density that affects the pore lining formation. This is consistent with the research conducted by Rahman *et. al.* [13] which stated the pore diameter decrease exponentially with the increasing of electrical potential.

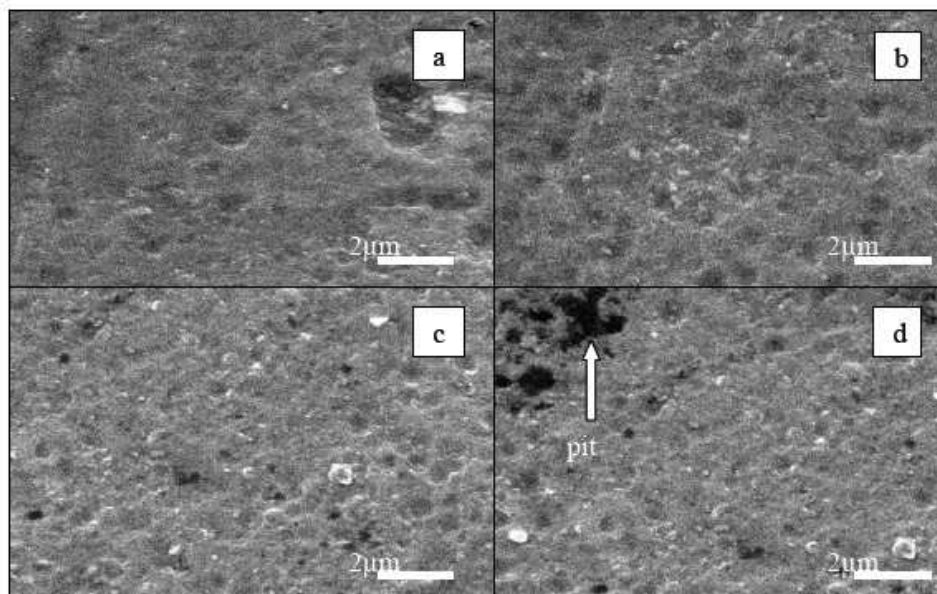


Figure 1 Surface morphology of the anodizing (a) 15V (b) 20V (c) 25V (d) 30V.

Meanwhile, there is an increase in specimen layer thickness after the anodizing process under an electrical potential with variations of (1.74; 4.36; 6.77; 7.47)  $\mu\text{m}$ , respectively. While the SEM on the cross-sectional side after anodizing process indicated that the pore size was relatively large and there is no relation one to another. Some new cavities appeared to form pores as shown in Figure 2. It was caused by the presence of oxygen as reported by Bouchamaet. *al.* From the study, it is stated that the cavity is formed due to the influence of oxygen presence during the process of pore formation [14].

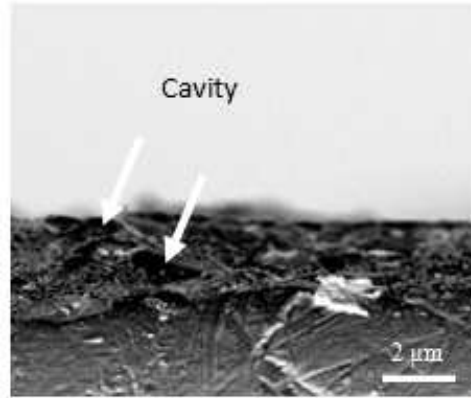


Figure2 Cross section after anodizing process.

When the electrical potential increase then the current density would increase and the chemical solubility rate for oxide layer during the anodizing process takes place [15]. It can be explained that during the process of anodizing aluminum, porous layer was formed by two processes, namely field-enhanced oxidation and field-enhanced aluminum oxide dissolution. At the pore side, there are two interfaces that include electrolyte-oxide and metal-oxide. Field-enhanced oxidation occurred at the interface where the pores position is close to the base containing oxygen ions  $\text{O}^{2-} / \text{OH}^-$  move from the electrolyte to the oxide layer, along the pores growth direction. At the same time,  $\text{Al}^{3+}$  metal ions moves from the metal to the interface solution / oxide and dissolved in the electrolyte. The metal ion transfer assisted by an electric current. This process was called the field-enhanced oxide dissolution. The intensity of electricity on the basis of pore area was greater than that on the walls. Aluminum will consume much higher electrical energy based on pores along with ongoing formation pore depth [16].

EDX particle components analysis in Figure 1 is shown in Table 1 which was the chemical composition of the surface after the anodizing process. In addition to Al, Si and Mg which are the main element that was dominant in AA6061, raised some new elements, namely O, C and Ti. O elements arising from the possibility of anion  $\text{PO}_4^{3-}$  which is part of the electrolyte. The existence of elements Ti here showed an increase in potential has been able to settle Ti at the anode during the process of decay of aluminum oxide. While the emergence of elements of C with a high enough value can be explained that during the process of data collection took place, aluminum was glued with graphite to ensure conductivity of specimen and their contacts to the specimen holder.

Table 1 Surface EDX analysis of anodized aluminum with different potential.

Element	15V		20V		25V		30V	
	Wt%	At%	Wt%	At%	Wt%	At%	Wt%	At%
<b>CK</b>	25.97	41.61	19.52	32.32	20.50	33.84	15.49	26.76
<b>OK</b>	11.19	13.45	16.34	20.32	15.23	18.88	15.48	20.08
<b>MgK</b>	01.74	01.38	02.01	01.65	01.78	01.45	01.82	01.56
<b>AlK</b>	61.04	43.54	61.87	45.61	62.20	45.71	67.04	51.54
<b>TiK</b>	00.06	00.02	00.25	00.11	00.29	00.12	00.16	00.07

Besides the EDX surface analysis, EDX analysis was also performed on the specimen cross section to determine the element (Al, Mg, Ti) content. Measurements were taken at four different locations, at a distance of 1, 3, 6 and 10  $\mu\text{m}$  from the surface of the specimen as shown in Figure 3. When a higher electrical potential is applied, as shown in the results of EDX, the Ti distribution

except formed on the surface, Ti was also found in 3 and 5  $\mu\text{m}$  from the surface. At the time of the oxide layer began to form through an electrochemical oxidation process in which the acid electrolyte  $\text{Al}_2\text{O}_3$  decay process occurs simultaneously with the formation of  $\text{Al}_2\text{O}_3$ . In an ideal condition, when the thickening layer of  $\text{Al}_2\text{O}_3$  pore base case, the barrier layer was formed relative constantly. It is proved that the balance occurred during the process of film formation of oxidation on the interface metal / oxide and the film layer decay at the interface oxide / electrolyte. However, the chemical solubility rate in oxide is much slower than the process of the oxide layer formation [17].

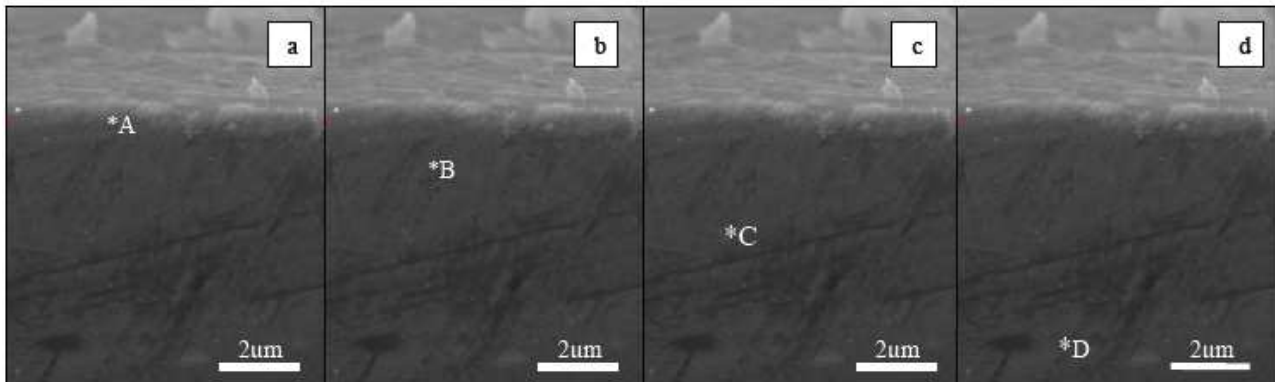


Figure 3 Cross section examination (a) 1  $\mu\text{m}$  (b) 3  $\mu\text{m}$  (c) 5  $\mu\text{m}$  (d) 10  $\mu\text{m}$  (note: \*: location of EDX analysis).

Based on Poinern *et al.*, the solubility mechanism takes place for weakening the chemical bonds of Al-O in the oxide lattice, that will cause the solubility of the interface film / electrolyte [5]. Meanwhile Oh and Thompson showed that the electrical area is the main reason for the transfer of ions through the barrier layer [16]. In the area of  $\text{OH}^-$  ions will move through the oxide to the metal interface / barrier layer. The process will react with  $\text{Al}^{3+}$  that will form the aluminum oxide. If the oxide formed by  $\text{OH}^-$  fewer than oxygen ion, the ion of  $\text{H}^+$  will be back on the film to the electrolyte. It showed the process of forming a continuous oxide layer.

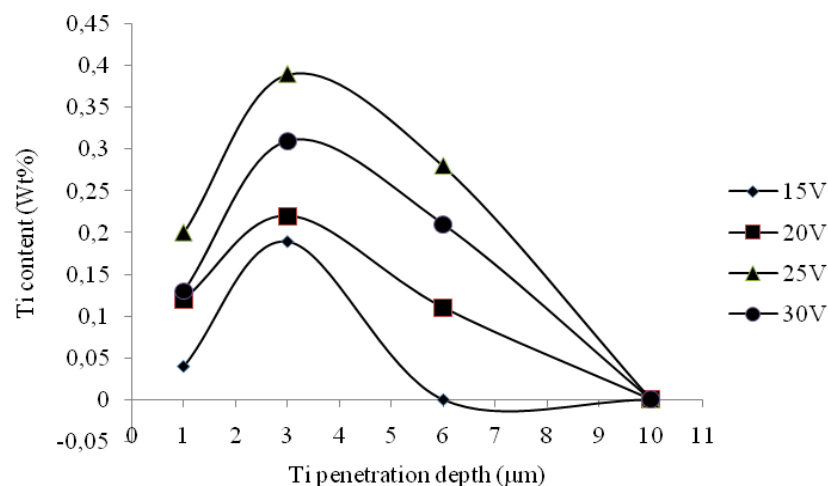


Figure 4 Comparison of titanium penetration measuring from the surface.

Meanwhile, if the other cathode used and not an inert metal, the system would change the balance in the region due to the high electrical potential implemented [18]. This phenomenon can be explained by the movement of titanium, where Ti move from the specimen surface when anodizing process takes place and the oxidation process continues. The high potential would start the oxidation process and involving titanium, which is positioned as a cathode and the oxidation state occur between the metal ions and the  $\text{O}^{2-}$  anions from the electrolyte solution. This has happened due to the electrical potential increase, would raise the solution temperature so that the cations and the anions in these conditions will move more aggressively. Increasing the electrical potential will

have a major influence on the pore shape and thickness. This shows that the ion transfer mechanism not only move the metal oxide layer, but also penetrate the pore walls as shown in Figure 4 [19].

### Conclusion

A simple way to make the oxide layer at a relatively low electrical potential and different cathode has been presented. The main findings of this study can be described as follows:

- Anodizing AA 6061 using a titanium cathode and low potential will reach the optimal value at potential of 25V, which gained 1.57 - 3.88  $\mu\text{m}$  pore size and layer thickness of 6.77  $\mu\text{m}$ . In addition to the deposit Ti on the surface of 0.29% Wt whereas titanium penetration pore layer can reach the value of 0.4% Wt at a depth of 5 $\mu\text{m}$ .
- Titanium when positioned as a cathode in the anodizing process to form an oxide layer of  $\text{TiO}_2$ . But not the entire surface of the anode coated by titanium oxide as the rate of speed of the formation of alumina is faster.

### References

- [1] T.Aerts, Th. Dimogerontakis, I.DeGraeve, J.Fransaer, H.Terryn, Surf. Coat. Technol. 201 (2007) p.7310
- [2] L.E. Fratila-Apachitei, I.Apachitei, J.Duszczuk, J. Appl. Electrochem. 36 (2006) p.481
- [3] J.M. Wheeler, J.A. Curran, S.Shresta, Surf.Coat. Technol. 207 (2012) p.480
- [4] W. Bensalah, M.Feki, M.Wery, H.F.Ayedi, Trans.Nonferrous.Met. Soc. China 21 (2011) p.1673
- [5] G.E.J.Poinern, N.Ali, D. Fawcett, Materials 4 (2011)p.487
- [6] J. Konmnskinieczny, K. Labisz, J. Wieczorek, L.A..Dobrzanski, Arch.Mater. Sci. Eng. 33 (2008)p.13
- [7] N.K.Allam, C.A. Grimes. Solar Ener.Mater.Solar Cells 92 (2008) p.1468
- [8] W. Aperador, A. Degado, J. Bautista, Intl. J. Electrochem. Sci. 8 (2013) p.9607
- [9] D.Zhang, Y.Gou, Y.:iu, X.Guo, Surf. Coat.Technol. 236 (2013) p.52
- [10]G.Q.Ding, R. Yang, J.N. Ding, N.Y. Yuan, Y.Y. Zhu, Nanoscale Research Lett.5(2010) p.1257
- [11] J. Martín, CV Manzano, O. Caballero-Calero, M. Martín-Gonzalez. ACS Appl.Mater.Interfac.5(2013) p.72
- [12] S.Ono, M..Masuko, Surf.Coat.Technol, 169-170(2003)p.139
- [13] M.M Rahman, E. Garcia-Caurel, A. Santos, L.F. Marsal, J. Pallares, J.Ferre-Borrull, Nanoscale Research Lett., 7(2012)p.474
- [14] L. Bouchama, N. Azzouz, N. Boukmouche, J.P.Chopart, A.L.Datin, Y.Bouznit, Surf.Coat. Technol. 235 (2013) p.676
- [15] H.Rezazadeh, M.Ebrahimzadeh, M.R.Z.Yam, World Acad. Sci. Engineer. Technol. 70 (2012) p.36
- [16] J.Oh, C.V. Thompson, Electrochim.Acta 56 (2011) p.4044
- [17] L.Zaraska, G.D.Sulka, J.Szeremeta, M.Jaskula, Electrochim.Acta 55 (2010) p.4377
- [18] G.E. Thompson, Thin Solid Film 297 (1997) p.192
- [19] Y-H. Chang, H-W. Lin, C.Chen, J.Electrochem. Soc. 159 (2012) D512-D517